FULL PAPER

Boosting Infrared Light Harvesting by Molecular Functionalization of Metal Oxide/Polymer Interfaces in Efficient Hybrid Solar Cells

*Giulia Grancini, R. Sai Santosh Kumar, Agnese Abrusci, Hin-Lap Yip, Chang-Zhi Li, Alex-K. Y. Jen, Guglielmo Lanzani, and Henry J. Snaith**

Hybrid solar cells based on light absorbing semiconducting polymers infiltrated in nanocrystalline TiO_2 electrodes, have emerged as an attractive concept, combining benefits of both low material and processing costs with well controlled nano-scale morphology. However, after over ten years of research effort, power conversion efficiencies remain around 0.5%. Here, a spectroscopic and device based investigation is presented, which leads to a new optimization route where by functionalization of the TiO_2 surface with a molecular electron acceptor promotes photoinduced electron transfer from a low-band gap polymer(poly[2,6-(4,4-bis-(2-ethylhexyl)-4H-cyclopenta[2,1-b;3,4-b0]dithiophene)-alt-4,7-(2,1,3-benzothiadia-zole)] (PCPDTBT) to the metal oxide. This boosts the infrared response and the power conversion efficiency to over 1%. As a further step, by "co-functionalizing" the TiO_2 surface with the electron acceptor and an organic dye-sensitizer, panchromatic spectral photoresponse is achieved in the visible to near-IR region. This novel architecture at the heterojunction opens new material design possibilities and represents an exciting route forward for hybrid photovoltaics.

1. Introduction

Hybrid solar cell architecture, based on semi-conducting polymers infiltrated into mesostructured metal oxide electrodes,[1–17] combines the high electron mobility, high electron affinity, non-toxicity, low-cost and physical and chemical stability of the metal oxide nanoparticles, with the good light absorbing and hole transporting properties of semiconducting polymers.[1–9] The metal oxide pre-ordered geometry ensures a high interfacial area[8] leading to well distributed exciton quenching sites, and a guaranteed bi-continuous network of pure phases providing effective charge transport paths. Importantly, metal oxides such as TiO_2 have extremely high dielectric constants, promising to overcome charge separation issues associated with Coulombically bound electron-hole pairs forming at all organic donor/acceptor interfaces.[18–20] Despite these "theoretical advantages" over all organic devices, to date these hybrid systems have underperformed with respect to competing concepts. The major limitation in these hybrid metal oxide/polymer solar cells has been previously thought to be related to ineffective pore infiltration of the semiconducting polymer into the mesoporous metal oxide electrode.[9,10] However, recent work has clearly demonstrated that this is not typically the case, and for instance poly(3-hexylthiophene) (P3HT) can infiltrate and collect charge effectively from mesoporous TiO_2 films as thick as 7 μm.[21] This therefore leaves inefficient photoinduced electron transfer at the polymer/TiO_2 interface[3,4] to be the most likely performance limiting mechanism. This could be related to the quality of the interface,[12,16] or due to the specific orientation of the polymer and electronic coupling between the excited state energy levels in the polymer and the conduction band states in the oxide. A further limitation in hybrid solar cells is due to the narrow photoresponse limited to light absorbed in the visible spectral region from the polymer, related to the polymers previously employed with ~1.9 eV band gaps.[9,11]

Solid-state dye-sensitized and extremely thin absorber solar cells have performed significantly better than polymer absorber based hybrid solar cells.[22,23] Recent reports of solid-state dye-sensitized solar cells, employing the light absorbing polymer P3HT as the hole conductor, have indeed delivered efficiencies over 3%.[9,11,21] However, for these systems, almost all the photocurrent originates from light absorbed in the dye absorber layer, and is not delivered from the polymer hole conductor.[21,24] An

G. Grancini, Dr. A. Abrusci, Dr. H. J. Snaith
Oxford University
Department of Physics
Clarendon Laboratory, Parks Road, Oxford, OX13PU, UK
E-mail: h.snaith1@physics.ox.ac.uk
G. Grancini, Prof. G. Lanzani
Dipartimento di Fisica
Politecnico di Milano
P.zza L. da Vinci 32, 20133 Milano, Italy
Dr. R. Sai Santosh Kumar, Prof. G. Lanzani
Center for Nano Science and Technology @Polimi
Istituto Italiano di Tecnologia
Via Pascoli 70/3 20133 Milano, Italy
H.-L. Yip, Dr. C.-Z. Li, Prof. A.-K. Y. Jen
Department of Materials Science and Engineering and Institute of Advanced Materials and Technology
University of Washington
Seattle, WA 98195, USA

DOI: 10.1002/adfm.201102360

inorganic extremely thin absorber concept employing Sb_2S_3 as the thin absorbing interlayer between mesoporous TiO_2 and P3HT hole-conductor has demonstrated over 5% power conversion efficiency.[25] However, once again, most of the photocurrent is delivered by the Sb_2S_3 absorber layer and not from the P3HT, evident from a dip in the spectral response in the region where the P3HT absorbs most strongly.[25] This literature indicates that electron transfer from photo-excited P3HT into TiO_2, or into an absorber layer, does not occur very effectively. An alternative route to generate charge from light absorbed in an organic semiconductor within a mesoporous oxide, is to employ resonant energy transfer to move the excitons from a wide band gap absorber within the pores, to a lower band gap dye sensitizer.[6,26] Recent reports of solid-state dye-sensitized solar cells (DSSCs) employing lower band gap dyes, in conjunction with P3HT as the hole-conductor, do indeed show photoaction from light absorbed in the polymer.[8,25,27]

A recent study by N. Humphry-Baker et al. clearly identifies that energy transfer can occur very efficiently from P3HT to a Zn Phalocyanine dye adsorbed to the surface of TiO_2.[28] However, this "energy transfer" approach limits the available possibly materials combinations to wide band gap hole-transporters in conjunction with low band gap dye-sensitizers, and requires very efficient low band gap sensitizers which are not currently developed for solid-state DSSCs. There is hence significant motivation to enable direct electron transfer from the photo-excited low band gap semiconducting polymers into mesoporous metal oxides.

Here, we perform a spectroscopic and device based investigation into hybrid solar cells composed of the low band gap polymer poly[2,6-(4,4-bis-(2-ethylhexyl)-4*H*-cyclopenta[2,1-*b*;3,4-*b'*]dithiophene)-*alt*-4,7-(2,1,3-benzothiadiazole)] (PCPDTBT) (Eg~ 1.45 eV) infiltrated into mesoporous TiO_2. We observe that photoinduced electron transfer at the TiO_2-PCPDTBT heterojunction does not compete with the natural decay of the exciton, resulting in extremely poor device performances under simulated sun light (J_{sc} ~ 0.23 mAcm^{-2}, η ~ 0.04%). To overcome this limitation of inefficient charge generation, we functionalize the TiO_2 surface with a fullerene based self-assembled monolayer (C_{60}-SAM), to make the oxide surface appear like an organic electron acceptor from the perspective of the polymer. The presence of electron acceptor molecules do indeed "photoactivate" the polymer; it drives efficient photo-induced electron transfer from the polymer to the C_{60}-SAM modified TiO_2 interface, resulting in over 10-fold enhancement in photocurrent and more than 20-fold enhancement in efficiency (η ~ 0.8%). To fine tune the energetic landscape at the heterojunction, specifically deepen the conduction band edge of TiO_2 to favor the forward electron transfer process, we add lithium bis(trifluoromethylsulfonyl)imide salt (Li-TFSI) to the system, which significantly enhances the current generation and efficiency in the hybrid devices to 1.1%.[9,11,17] As a final modification, we "co-functionalize" the TiO_2 surface with a mixed monolayer of C_{60}-SAM and a yellow dye-sensitizer (D131), to deliver a panchromatic photoresponse. Notably, the optimized devices deliver external quantum efficiencies of over 30% at 700 nm (corresponding to PCPDTBT absorption), short-circuit photocurrents of 8 mAcm^{-2} under AM1.5 simulated sun light of 100 mW/cm^{-2} and power conversion efficiencies of up to 1.4%, representing a step in performance for "polymer absorber" based mesoscopic hybrid solar cell.

2. Results and Discussion

The structure of PCPDTBT is shown in **Figure 1**a. The close to ideal optical band gap of PCPDTBT is ~1.4 eV, leading to improved light harvesting in the near-infrared region,[29] combined with the high hole mobility of 2×10^{-2} cm^2 V^{-1} s^{-1} and easy processability[29–32] have made this material a good candidate for photovoltaic applications.[29–35] The absorption spectrum of the PCPDTBT is shown by the solid line in Figure 1a: it peaks around 700 nm, with a secondary feature around 400 nm. Figure 1c shows the architecture of the hybrid devices presented in this study. They consist of a mesoporous layer of TiO_2, serving as the electron acceptor, infiltrated with the polymer phase, acting as light absorber and hole conducting material (see Supporting Information for further details in device fabrication). Further modifications include functionalizing the surface of the TiO_2 with a fullerene based self assembled monolayer (C_{60}-SAM) containing a carboxylic acid terminated anchoring group, and also co-functionalizing with a mixed monolayer of C_{60}-SAM and an indolene based dye-sensitizer, termed D131.

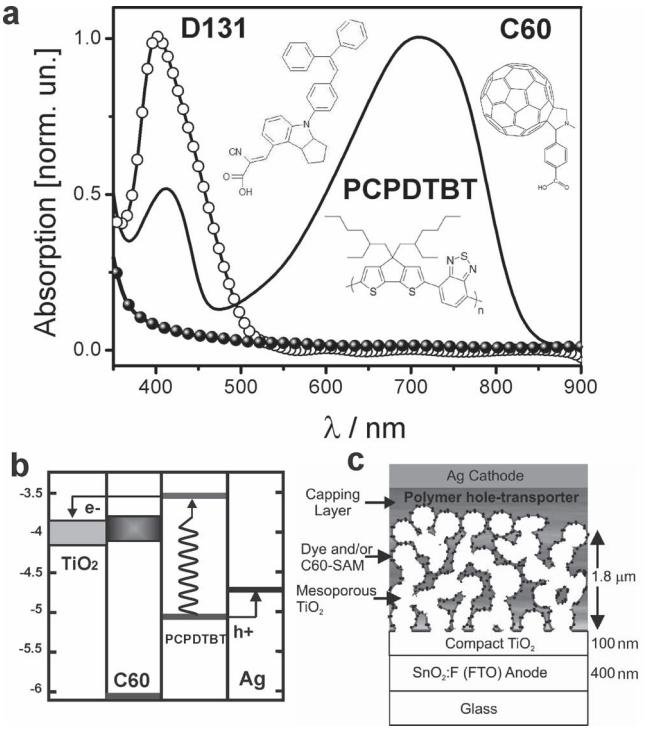

Figure 1. a) Absorption spectra of PCPDTBT (solid line), C_{60}-SAM (full dots) and D131 dye (open circles) functionalized upon mesoporous TiO_2. The chemical structures are inset. b) Schematic diagram of energy levels of TiO_2, PCPDTBT and C_{60}-SAM. The thick line for the C_{60}-SAM and TiO_2 LUMO level and conduction band respectively represent the uncertainty of positioning the C_{60}-SAM energy level, as discussed in the text. c) Cartoon of the architecture of the fabricated hybrid solar cell based on a mesoporous TiO_2 film co-functionalized with the C_{60}-SAM and dye-sensitizer and infiltrated with the polymer.

The chemical structure of the C_{60}-SAM and D131 are also shown in Figure 1a and the synthesis procedure reported elsewhere.[36–40] The C_{60}-SAM exhibits a negligible absorption in the visible spectral region, with an onset at around 350 nm, as shown in Figure 1a. Figure 1b shows the approximate energetic landscape of various materials, further analysis on the positioning of the C_{60}-SAM energy levels is presented below (see Supporting Information for details).

The solar cell characteristics of PCPDTBT/TiO_2 hybrid solar cells are shown in **Figure 2**, measured under simulated AM 1.5G solar conditions at 100 mWcm^{-2} intensity. The current density-voltage (*J–V*) characteristic reveals good rectification and diodic behavior, however, the photocurrent and overall solar power conversion efficiency are extremely poor, only 0.2 mA/cm^2 with 0.04% respectively. As indicated by the external quantum efficiency (EQE), the contribution to the photocurrent from light harvested in the polymer is extremely low (less then 1% EQE). In order to elucidate the low photocurrent generation in this system we employ ultrafast transient absorption (TA) spectroscopy, as a powerful technique to monitor the electron transfer dynamics.[41–43] Figure 2d shows the TA spectrum of TiO_2/PCPDTBT sample upon excitation at 780 nm, corresponding to the main PCPDTBT absorption peak. The positive fractional transmission signal (ΔT/T) from 650 nm to near IR (extending beyond the probe spectral range) is attributed to photobleaching (PB) and stimulated emission (SE), while the negative band at shorter wavelength (<560 nm) is due to photoinduced absorption (PA_1) of the singlet exciton. All these features are related to transitions from the first excited singlet state, as indicated by the energy levels diagram in Figure 2c and the dynamics resemble the ones of a neat PCPDTBT film.[42,43] After few tens of ps a tiny negative band appears around 900 nm, attributed to polaron absorption (PA_2). However, the signal is extremely small, indicating that a very small population of charges are created after exciton separation at the TiO_2 interface. The results above demonstrate that photoexcited excitons undergo negligible electron transfer to the TiO_2. Here, the electronic energy levels should be suitably offset to enable forward electron transfer, thus the lack of charge generation suggests poor electronic coupling between the lowest unoccupied molecular orbital (LUMO) level of the polymer and the conduction band states in TiO_2. On reflection, this is not entirely surprising: If the polymer has a stronger tendency to form inter chain π-orbital interactions than with the oxide surface, then the polymer may predominantly contact the oxide surface side-on or via the aliphatic chains, minimizing the electronic orbital overlap between the polymer and the metal oxide. In contrast, organic-organic heterojunctions tend to quench excitons very effectively, provided there is a suitable LUMO level energy offset.[44–46] Often for organic-organic heterojunctions, the electronic coupling is so strong that specific interface states, such as exciplexes, and ground state charge transfer complexes are created, indicating good compatibility.[18,44–47]

In order to enhance the device performance here we functionalize the TiO_2 surface with a fullerene based (C_{60}-SAM) organic electron acceptor, as used very effectively in bulk heterojunction solar cells.[18,19] Moreover, C_{60}-SAM modifiers with carboxylic acid anchoring groups have been used previously in inverted bulk heterojunction based devices to both improve the vertical phase segregation of the de-mixed polymer blend, and to also promote forward electron transfer from excitons in the polymer to ZnO electrodes.[36–40] Here, our ensuing "functionalized" hybrid solar cells operate significantly better than the basic device structure. As measured under simulated AM 1.5 solar illumination at 100 mW cm^{-2}, the C_{60}-SAM functionalization increases the photocurrent by about one order of magnitude from 0.23 to 2 mAcm^{-2} with an open-circuit voltage of 0.64 V, and efficiency as high as ~0.8%. Though this is already a significant breakthrough for polymer absorber based mesoscopic hybrid solar cells, PCPDTBT has the potential to generate over 25 mA cm^{-2}, if it could convert the solar photons to electrons with 90% efficiency. Hence there clearly remain major losses in this system. It is possible that the energetic of the system are not ideal. Assuming the offset between the PCPDTBT and C_{60} is suitable (as occurring in bulk heterojunctions) then, if the LUMO of the C_{60}-SAM is deeper, or not sufficiently higher than the conduction band edge of the TiO_2, this may result in ineffective forward electron transfer. It is very difficult to estimate the relative offset of LUMO and conduction band levels: firstly, there is no guaranteed and universal conversion between electrochemical measurements

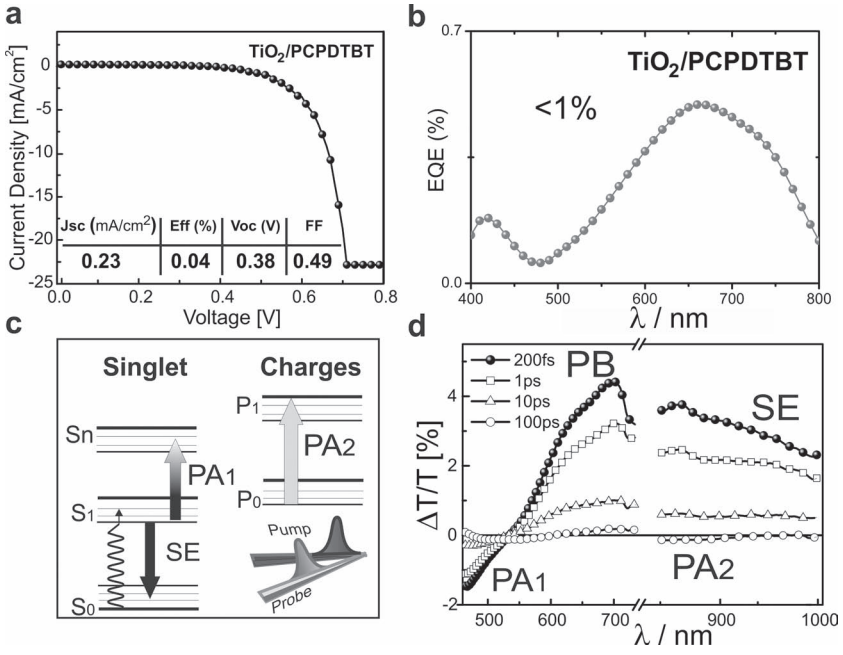

Figure 2. Solar cell performance and photophysicsof a for a TiO_2/PCPDTBT based device. a) Photocurrent–voltage curve measured under AM 1.5G simulated sun light of 100 mWcm^{-2}, the inset is a table showing the device performance parameters. b) external quantum efficiency spectrum. c) Scheme of electronic levels of the PCPDTBT and relative transition. d) Pump-probe spectrum of TiO_2/PCPDTBT sample collected at different pump-probe delay, from 200 fs to 100 ps, as indicated in the legend.

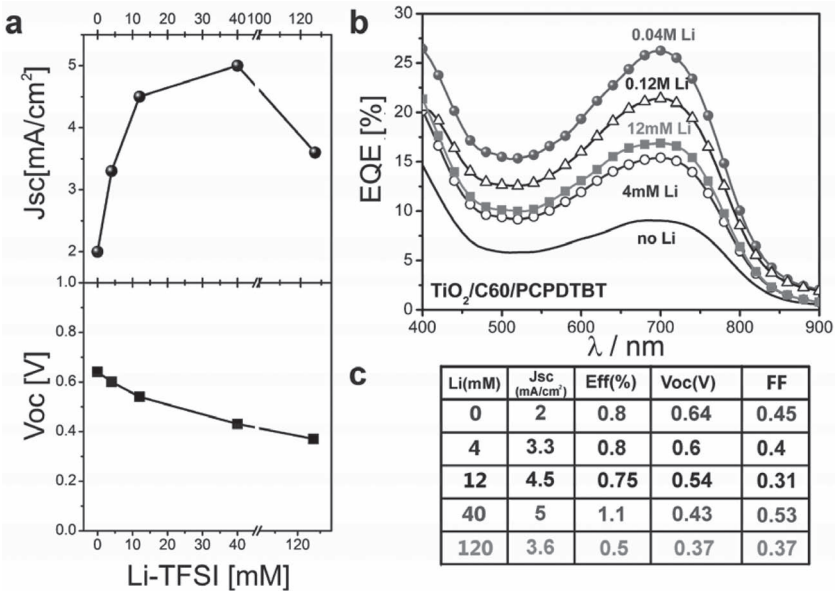

c

Li(mM)	Jsc (mA/cm²)	Eff(%)	Voc(V)	FF
0	2	0.8	0.64	0.45
4	3.3	0.8	0.6	0.4
12	4.5	0.75	0.54	0.31
40	5	1.1	0.43	0.53
120	3.6	0.5	0.37	0.37

Figure 3. a) Short-circuit current density (J_{sc}) (top panel, solid-circles) and open-circuit voltage (V_{oc}) (bottom panel, solid-squares) for functionalized hybrid solar cells (TiO_2/C_{60}-SAM/PCPDTBT) measured under AM1.5 simulated sun light as a function of Li-TFSI concentration in the coating solution. b) Spectral response of TiO_2/C_{60}-SAM/PCPDTBT based devices with no Li-TFSI (black solid line) and with the addition of increasing Li-TFSI content. c) Table showing the device performance parameters, measured under AM 1.5G simulated sun light of 100 mW cm^{-2}.

(ferrocene/ferrocenium, Fc/Fc+) to absolute energy. Even if this was unambiguous, when two materials make contact there can very easily be up to 0.5 eV shift in the relative surface energy at the interface, due to some degree of charge transfer. Ultraviolet photoelectron spectroscopy offers a direct measurement at real interfaces, however, this is performed under ultra high vacuum and is likely to differ from that in the constricted device. We have performed cyclic voltammetry (CV) measurements on compact TiO_2 and that functionalized within the C_{60}-SAM (reported in the Supporting Information). We find that there is a 50 meV negative shift in reduction onset of the functionalized surface, with respect to the bare TiO_2, as measured in Fc/Fc^+. This would suggest that the energy level offset between the C_{60}-SAM and TiO_2 are almost perfectly set. However, there are a number of reasons why this still may not be the case: i) it may be necessary to have more than 50 meV offset to ensure effective forward electron transfer, following exciton ionization at the polymer C_{60} interface; ii) the reduction onset of TiO_2, as measured by CV, may represent filling of the sub-band gap states, rather than the conduction band level; iii) the surface potential of TiO_2 is known to be extremely sensitive to its environment, i.e., level of protonation, presence of ionic species, and the surface potential in Fc/Fc^+ may be considerably different to in the fabricated solar cell. In order to asses if there is a requirement to shift the TiO_2 conduction band level, we have coated the functionalized TiO_2 surface with Li-TFSI prior to deposit the PCPDTBT. Lithium ions are "potentially determining"for TiO_2, resulting in a positive shift, thus deepening the TiO_2 conduction band level with respect to the C_{60}-SAM.[9,11,17] The evolution of the short-circuit current and open-circuit voltage for functionalized hybrid solar cells with increasing Li-TFSI concentrations is presented in **Figure 3**a. As expected, the open-circuit voltage drops monotonically with increasing Li-TFSI concentration. Quite remarkably, the short-circuit photocurrent increases by a factor of 3 up to 5.5 mA cm^{-2} over the range studied and the efficiency rises to 1.1%. Though this is not a staggeringly high efficiency in comparison to other more developed organic solar cells, this is a remarkable milestone considering that, to the best of our knowledge, it is the first time that mesoporous metal oxide hybrid solar cells, employing the polymer as the sole absorber, have delivered over 1% power conversion efficiency. We note that there is a fluctuation in FF with changing Li-TFSI content, however this does not follow a trend. The presence of the ions does alter the film forming properties of the polymer, and this may be partly responsible for this relatively large variation. In Figure 3b, we show the photovoltaic action spectra for the same devices which were tested under the simulated sun light, exhibiting a maximum EQE approaching 30% at 700 nm.

The motivation for addition of the Li-TFSI to the system was to improve the forward electron transfer from the C_{60}-SAM to the TiO_2. In order to understand the processes in more detail, here we perform transient absorption spectroscopy studies of the system, the results are presented in **Figure 4**. We photoexcite the low band-gap polymer using a 780 nm pump pulse at low pump energy (less than 50 nJ) and we monitor the charge generation dynamics at an ultrafast time scale. Figure 4a and 4b show the TA measurements on devices without and with Li-TFSI treatment, respectively. Firstly, in comparison to the unmodified PCPDTBT-TiO_2 interface (Figure 2d), the C_{60} functionalized devices exhibit strikingly different TA characteristics, both with and without Li-TFSI, particularly in the near IR probe spectral region. Considering the device without Li-TFSI (Figure 4a) the SE (peaking at 900 nm) is rapidly quenched within 10 ps, compared with the singlet lifetime in the neat polymer of a few hundred ps. We assign the PA band around 900 nm as a fingerprint of charge population in PCPDTBT.[42,43] From our results it is clear that ultrafast charge generation only occurs when the C_{60}-SAM is employed, as supported by the comparison to the bare TiO_2/PCPDTBT devices. Figure 4b presents the analogous results on the devices processed with optimal Li-TFSI concentration. The PA bands related to charge formation, responsible for the good photocurrent generation, are still evident. Indeed, the charge band formation around 900 nm probe wavelength, appears to be even faster: the charges are instantaneously photogenerated, since the PA signal is negative from the earliest time. This indicates that ultrafast charge separation occurs in presence of Li ions, in contrast to the slow evolution of the charge signal without any Li salts. In this case (see Figure 4b) no SE from singlets is detected, thus indicating that almost 100% of the photo-excited singlets efficiently separate into charges. However, when photo-exciting the polymer

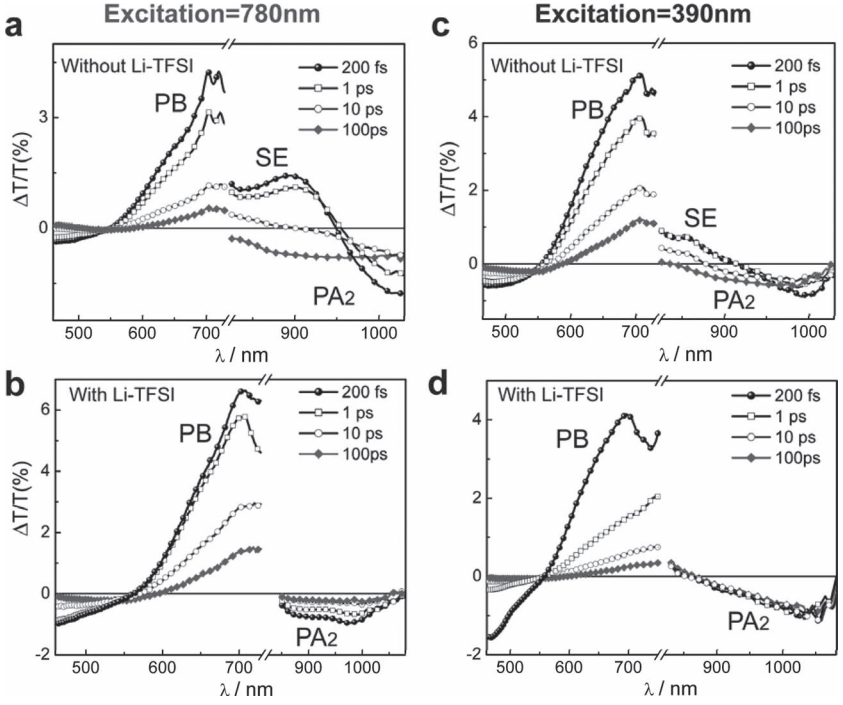

Figure 4. Ultrafast transient absorption measurements of a,c) TiO_2/C_{60}-SAM/PCPDTBT and b,d) TiO_2/Li-TFSI/C_{60}-SAM/PCPDTBT at a,b) 780 nm and c,d) 390 nm pump wavelength respectively, collected at different pump-probe delays from 200 fs to 100 ps as indicated in the legend. Pump Energy <50 nJ.

at 780 nm, an initial fast decay of the charges occurs, possibly due to a geminate recombination between electrons on the C_{60} and holes in the polymer. In order to obtain a more complete picture on the ultrafast charge generation process we tune the pump wavelength to 390 nm, resonant to the higher energy PCPDTBT absorption peak. Figure 4c and d show the results on the devices processed without and with Li salts. Without Li-TFSI (Figure 4c) the results match the TA measurements obtained upon exciting the polymer at 780 nm, thus showing a broad PA band at near IR spectral region, as previously assigned to charge generation. When Li ions are added (Figure 4d) the mechanism is still the same, but a faster and more efficient charge generation seems to occur, especially evident at this excitation wavelength.

Though pumping at both 390 and 780 nm almost exclusively excites the polymer, pumping at 780 nm charges are instantaneously generated, but their signal undergoes a decay to about 30% of its initial value within a few tens of ps. In contrast, pumping at 390 nm results in little decay over the measurement window of 100 ps. Our best hypothesis is that when pumping at 780 nm, the electrons temporarily reside upon the C_{60}-SAM molecules thus allowing geminate recombination with the hole residing on the polymer. However, for the 390 nm pump, "hot electron transfer" may occur with the electron "bridged" directly through the C_{60}-SAM into the TiO_2 (see Figure S0 in Supporting Information that compares the PA dynamics selected at 960 nm probe wavelength upon 390 nm and 780 nm excitation wavelength). The argument follows similar considerations to the Onsager model for charge separation:[18,48] the hot charge pairs thermalise at larger distances, thus increasing the likelihood for complete charge separation. For organic PV, the cristalinity of the fullerene domain appears to play a critical role in charge separation, indicating that electron transport away from the charge generating interface is a requirement. In the case of photoexciation at 780nm, the electrondoes not have sufficient kinetic energy to transfer "instantaneously" into the TiO_2 prior to thermalization, hence it is susceptible to geminate recombination. Notably the external quantum efficiency, in comparison to the light absorption, is much higher at 400 nm than at 700 nm, consistent with improved charge separation. We note that when combined with $PC_{60}BM$ in bulk heterojunction polymer solar cells, PCPDTBT can generate photocurrent very efficiently, suggesting that the structural and electronic configuration of the polymer-acceptor interface is close to ideal. However, here, this may be influenced by the confinement of the polymer within the mesoporous TiO_2 network, and the tethering of the C_{60} to the titania surface. To completely understand charge generation and to understand and improve the device manufacture and operation, further structural studies of the polymer electron acceptor interface within the mesoporous network are required.

Due to the absorption profile of PCPDTBT, there is a significant dip in response in the mid visible region. In bulk heterojunction solar cells this is "filled" to a certain extent by employing a light absorbing electron acceptor, $PC_{70}BM$.[42,43,49] This has motivated us to investigate the possible advantages of "co-functionalizing" the surface with a mixed monolayer of both C_{60}-SAM and light absorbing dye molecules. We have optimized the co-functionalization of the TiO_2 surface with a mixed layer of organic indolene dye (D131) and C_{60}-SAM. **Figure 5**a,b shows the obtained spectral response and current voltage output measured under simulated sun light respectively, comparing three different device architecture.

From the spectral response measurements, the co-functionalized device has significantly increased the response in the visible region of the spectrum due to light absorbed in the dye-sensitizer. Notably, the co-functionalized device without any Li-TFSI already shows good performances (J_{sc} = 4.3 mA/cm^2, Efficiency = 1.2%). With the presence of Li the photoaction is further enhanced with the EQE approaching 50% in the visible region and over 30% from near IR, related respectively to dye and polymer absorption contributions. The highest photocurrent for the co-functionalized device is over 8 mAcm^{-2} and the corresponding power conversion efficiency is 1.4%. These devices were around 1.5 μm in thickness, which we found to be optimum. The photocurrent generated in this co-functionalized hybrid system is comparable to the best performing solid-state dye sensitized-solar cells (~10 mAcm^{-2})[22,27,50,51] and there is clearly massive scope for significant enhancement.

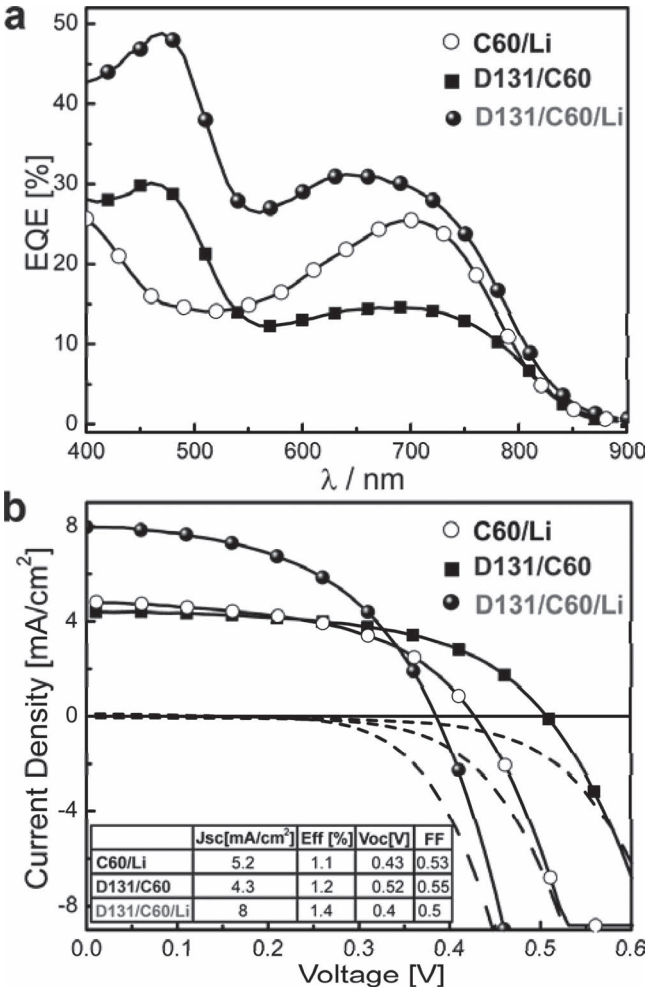

Figure 5. a) External quantum efficiency measurements and b) Photocurrent-voltage curves for a TiO_2/C_{60}/Li-TFSI/PCPDTBT device (open dots line), TiO_2/D131/C_{60}SAM/PCPDTBT device (full square line) and TiO_2/D131/C_{60}SAM/Li-TFSI/PCPDTBT device (full dot line) measured under AM 1.5G simulated sun light of 100 mWcm^{-2}. In the table inset of (b) shows the device performance parameters.

Furthermore, the near IR contribution from the polymer is more significant than that obtained from near-IR dyes in solid-state dye-sensitized solar cells.[25,26,50,51] The challenge is to engineer the interface[13–16,40] between the oxide and the polymer to enable "instantaneous" electron transfer, while also retaining a high open-circuit voltage.

3. Conclusions

In summary, we have clearly identified that electron transfer from the photo-excited polymer to the metal oxide, is the main limitation in polymer absorber based hybrid solar cells. To overcome this limitation, we have presented a strategy whereby the surface of the mesoporous oxide is functionalized with a molecular electron acceptor, which acts an intermediary species, electronically coupling the semiconducting polymer to the metal oxide. Through this route we have obtained an order of magnitude increase in the photocurrent in the solar cells employing a low band gap polymer PCPDTBT. Additionally, by tuning the surface potential of the metal oxide with the addition of Li-TFSI, the photocurrent is further increased, delivering hybrid solar cells with over 30% external quantum efficiency from light absorbed in near IR region in the polymer phase. Finally, in order to achieve a panchromatic photoresponse, we have also introduced a new concept of "co-functionalization" of the surface with both dye-sensitizer and electron accepting components, which results in a further increase in photocurrent. This work represents a key step for polymer absorber based hybrid solar cells, opening significant possibilities for new molecular design and system optimization.

Supporting Information

Supporting Information is available from the Wiley Online Library or from the author.

Acknowledgements

This work was part funded by EPSRC. We thank Dr. Annamaria Petrozza for helpful discussions.

Received: October 2, 2011
Revised: December 5, 2011
Published online: February 22, 2012

[1] H. J. Snaith, A. J. Moule, C. Klein, K. Meerholz, R. H. Friend, M. Grätzel, *Nano Lett.* **2007**, *7*, 3372.
[2] E. Arici, N. S. Sariciftci, D. Meissner, in *Encyclopedia of Nanoscience and Nanotechnology*, Vol. 3, 929 (Ed. H. S. Nalwa) American Scientific Publishers, California, USA, **2004**.
[3] K. M. Coakley, M. D. McGehee, *Appl. Phys. Lett.* **2003**, *83*, 3380.
[4] M. D. McGehee, *Mater. Res. Bull.* **2009**, *34*, 95.
[5] M. Grätzel, *J. Photochem. Photobiol. C* **2003**, *4*, 145.
[6] B. E. Hardin, E. T. Hoke, P.B. Armstrong, J. H. Yum, P. Comte, T. Torres, J. M. J. Fréchet, M. K. Nazeeruddin, M. Grätzel; M. D. McGehee, *Nat. Photonics* **2009**, *3*, 406.
[7] S. Günes, H. Neugebauer, N. S. Sariciftci, *Chem. Rev.* **2007**, *107*, 1324.
[8] G. K. Mor, S. Kim, M. Paulose, O. K. Varghese, K. Shankar, J. Basham, C. A. Grimes, *Nano Lett.* **2009**, *9*, 4250.
[9] K. J. Jiang, K. Manseki, Y. H. Yu, N. Masaki, K. Suzuki, Y. L. Song, S. Yanagida, *Adv. Funct. Mater.* **2009**, *19*, 2481.
[10] K. M. Coakley, Y. Liu, M. D. McGehee, K. L. Frindell, G. D. Stucky, *Adv. Funct. Mater.* **2003**, *13*, 301.
[11] R. Zhu, C. Y. Jiang, B. Liu, S. Ramakrishna, *Adv. Mater.* **2009**, *21*, 994.
[12] P. Ravirajan, S. A. Haque, J. R. Durrant, D. D. C. Bradley, J. Nelson, *Adv. Funct. Mater.* **2005**, *15*, 609.
[13] H. J. Snaith, M. Grätzel, *Appl. Phys. Lett.* **2006**, *89*, 262114.
[14] C. Goh, S. R. Scully, M. D. McGehee, *J. Appl. Phys.* **2007**, *101*, 114503.
[15] Y. Y. Lin, T. H. Chu, S. S. Li, C. H. Chuang, C. H. Chang, W. F. Su, C. P. Chang, M. W. Chu, C. W. Chen, *J. Am. Chem. Soc.* **2009**, *131*, 3644.
[16] J. Bouclé, S. Chyla, M. S. P. Shaffer, J. R. Durrant, D. D. C. Bradley, J. Nelson, *Adv. Funct. Mater.* **2008**, *18*, 622.

[17] A. Abrusci, R. S. S. Kumar, M. Al-Hashimi, M. Heeney, A. Petrozza, H. J. Snaith, *Adv. Funct. Mater.* **2011**, *21*, 2571.
[18] T. M. Clarke, J. R. Durrant, *Chem. Rev.* **2010**, *110*, 6736.
[19] J. Peet, A. J. Heeger, G. C. Bazan, *Acc. Chem. Res.* **2009**, *42*, 1700.
[20] C. Risko, M. D. McGehee, J. L. Bredas, *Chem. Sci.* **2011**, *2*, 1200.
[21] A. Abrusci, I.-K. Ding, M. Al-Hashimi, T. Segal-Peretz, M. D. McGehee, M. Heeney, G. L. Frey, H. J. Snaith, *Energy Environ. Sci.* **2011**, *4*, 3051.
[22] J. Burschka, A. Dualeh, F. Kessler, E. Baranoff, N. L. Cevey-Ha, C. Yi, M. K. Nazeeruddin, M. Grätzel, *J. Am. Chem. Soc.* **2011**, *133*, 18042.
[23] J. A. Chang, J. H. Rhee, S. H. Im, Y. Hui Lee, H.-j. Kim, S. I. Seok, Md. K. Nazeeruddin, M. Grätzel, *Nano Lett.* **2010**, *10*, 2609.
[24] S. Wang, X. Zhang, G. Zhou, Z.-S. Wang, *Phys. Chem. Chem. Phys.* **2012**, *14*, 816.
[25] H. J. Lee, H. C. Leventis, S. A. Haque, T. Torres, M. Graetzel, M. K. Nazeeruddin, *J. Power Sources* **2011**, *196*, 596.
[26] K. Driscoll, J. Fang, N. Humphry-Baker, T. Torres, W. T. S. Huck, H. J. Snaith, R. H. Friend, *Nano Lett.* **2010**, *10*, 4981.
[27] S. J. Moon, E. Barnhoff, S. H. Zakeeruddin, C.-U. Yeh, E. W. G. Diau, M. Graetzel, K. Sivula, *Chem. Commun.* **2011**, *47*, 8244.
[28] N. Humphry-Baker, K. Driscoll, A. Rao, T. Torres, H. J. Snaith, R. H. Friend, *Nano Lett.* **2012** DOI: 10.1021/nl203377r.
[29] D. Mühlbacher, M. Scharber, M. Morana, Z. Zhu, D. Waller, R. Gaudiana, C. J. Brabec, *Adv. Mater.* **2006**, *18*, 2884.
[30] C. Soci, I. Hwang, D. Moses, Z. Zhu, D. Waller, R. Gaudiana, C. J. Brabec, A. J. Heeger, *Adv. Funct. Mater.* **2007**, *17* (4), 632.
[31] M. C. Scharber, M. Koppe, J. Gao, F. Cordella, M. A. Loi, P. Denk, M. Morana, H. J. Egelhaaf, K. Forberich, G. Dennler, R. Gaudiana, D. Waller, Z. Zhu, X. Shi, C. J. Brabec, *Adv. Mater.* **2010**, *22*, 367.
[32] M. Morana, M. Wegscheider, A. Bonanni, N. Kopidakis, S. Shaheen, M. Scharber, Z. Zhu, D. Waller, R. Gaudiana, C. J. Brabec, *Adv. Funct. Mater.* **2008**, *18*, 1757.
[33] J. Peet, J. Y. Kim, N. E. Coates, W. L. Ma, D. Moses, A. J. Heeger, G. C. Bazan, *Nat. Mater.* **2007**, *6*, 497.
[34] Y. Liang, Z. Xu, J. Xia, S. T. Tsai, Y. Wu, G. Li, C. Ray, L. Yu, *Adv. Mater.* **2010**, *22*, E135.
[35] J. K. Lee, W. L. Ma, C. J. Brabec, J. Yuen, J. S. Moon, J. Y. Kim, K. Lee, G. C. Bazan, A. J. Heeger, *J. Am. Chem. Soc.* **2008**, *130*, 3619.
[36] S. K. Hau, H. L. Yip, O. Acton, N. S. Baek, H. Maa, A. K. Y Jen, *J. Mater. Chem.* **2008**, *18*, 5113.
[37] S. K. Hau, Y. J. Cheng, H. L. Yip, Y. Zhang, H. Ma, A. K. Y. Jen, *Appl. Mater. Interfaces* **2010**, *2*, 1892.
[38] H. L. Yip, S. K. Hau, N. S. Baek, H. Ma, A. K. Y. Jen, *Adv. Mater.* **2008**, *20*, 2376.
[39] H. L. Yip, S. K. Hau, N. S. Baek, A. K. Y. Jen, *Appl. Phys. Lett.* **2008**, *92*, 193313.
[40] Y. Vaynzof, D. Kabra, L. Zhao, P. K. H. Ho, A. T. S. Wee, R. H. Friend, *Appl. Phys. Lett.* **2010**, *97*, 033309.
[41] J. Cabanillas-Gonzalez, G. Grancini, G. Lanzani, *Adv. Mater.* **2011**, DOI: 10.1002/adma.201102015.
[42] W. Hwang, C. Soci, D. Moses, Z. Zhu, D. Waller, R. Gaudiana, C. J. Brabec, A. J. Heeger, *Adv. Mater.* **2007**, *19*, 2307.
[43] W. Hwang, S. Cho, J. Y. Kim, K. Lee, N. E. Coates, D. Moses, A. J. Heeger, *J. Appl. Phys.* **2008**, *104*, 0337061.
[44] D. Veldman, O. Ipek, S. C. J. Meskers, J. Sweelssen, M. M. Koetse, S. C.Veenstra, J. M. Kroon, S. S. van Bavel, J. Loos, R. A. J. Janssen, *J. Am. Chem Soc.* **2008**, *130*, 7721.
[45] Y. S. Huang, S. Westenhoff, I. Avilov, P. Sreearunothai, J. M. Hodgkiss, C. Deleener, R. H. Friend, D. Beljonne, *Nat. Mater.* **2008**, *7*, 483.
[46] C. Morteani, A. S. Dhoot, J. S. Kim, C. Silva, N. C. Greenham, C. Murphy, E. Moons, S. Ciná, J. H. Burroughes, R. H. Friend, *Adv. Mater.* **2003**, *15*, 1708.
[47] G. Grancini, D. Polli, D. Fazzi, J. Cabanillas-Gonzalez, G. Cerullo, G. Lanzani, *J. Phys. Chem. Lett.* **2011**, *2*, 1099.
[48] D. Hertel, H. Bässler, *Chem. Phys. Chem.* **2008**, *9*, 666.
[49] S. H. Park, A. Roy, S. Beaupré, S. Cho, N. Coates, J. S. Moon, D. Moses, M. Leclerc, K. Lee, A. J. Heeger, *Nat. Photonics* **2009**, *3*, 297.
[50] N. Cai, S. J. Moon, L. C. Ha, T. Moehl, R. Humphry-Baker, P. Wang, S. M. Zakeeruddin, M. Grätzel, *Nano Lett.* **2011**, *11*, 1452.
[51] P. Y. Reddy, L. Giribabu, C. Lyness, H. J. Snaith, C. Vijaykumar; M. Chandrasekharam, M. Lakshmikantam, J. H. Yum, K. Kalyanasundaram, M. Grätzel, M. K. Nazeeruddin, *Angew. Chem.* **2006**, *45*, 1.